

**GSFC JPSS CMO  
December 5, 2011  
Released**

**Joint Polar Satellite System (JPSS) Ground Project  
Code 474  
474-00052**

**Joint Polar Satellite System (JPSS)  
VIIRS Ice Surface Temperature  
Algorithm Theoretical Basis Document  
(ATBD)**

**For Public Release**

The information provided herein does not contain technical data as defined in the International Traffic in Arms Regulations (ITAR) 22 CFC 120.10. This document has been approved For Public Release to the NOAA Comprehensive Large Array-data Stewardship System (CLASS).



National Aeronautics and  
Space Administration

**Goddard Space Flight Center  
Greenbelt, Maryland**



This page intentionally left blank.



# **Joint Polar Satellite System (JPSS) VIIRS Ice Surface Temperature Algorithm Theoretical Basis Document (ATBD)**

## **Electronic Signature Page**

### **Prepared By:**

Neal Baker  
JPSS Data Products and Algorithms, Senior Engineering Advisor  
(Electronic Approvals available online at ([https://jpssmis.gsfc.nasa.gov/mainmenu\\_dsp.cfm](https://jpssmis.gsfc.nasa.gov/mainmenu_dsp.cfm) )

### **Approved By:**

Heather Kilcoyne  
DPA Manager  
(Electronic Approvals available online at ([https://jpssmis.gsfc.nasa.gov/mainmenu\\_dsp.cfm](https://jpssmis.gsfc.nasa.gov/mainmenu_dsp.cfm) )

**Goddard Space Flight Center  
Greenbelt, Maryland**

This page intentionally left blank.

## Preface

This document is under JPSS Ground AERB configuration control. Once this document is approved, JPSS approved changes are handled in accordance with Class I and Class II change control requirements as described in the JPSS Configuration Management Procedures, and changes to this document shall be made by complete revision.

Any questions should be addressed to:

JPSS Ground Project Configuration Management Office  
NASA/GSFC  
Code 474  
Greenbelt, MD 20771

This page intentionally left blank.

## Change History Log

Revision	Effective Date	Description of Changes (Reference the CCR & CCB/ERB Approve Date)
Original	04/22/2011	<b>474-CCR-11-0067:</b> This version baselines D43761, VIIRS Ice Surface Temperature Algorithm Theoretical Basis Document ATDB (ref Y2405), Rev B, dated 12/22/2010, as a JPSS document, version Rev -. This is the version that was approved for NPP launch. Per NPOESS CDFCB - External, Volume V – Metadata, doc number D34862-05, this has been approved for Public Release into CLASS. This CCR was approved by the JPSS Algorithm ERB on April 22, 2011.

This page intentionally left blank.

Northrop Grumman Aerospace Systems  
One Space Park  
Redondo Beach, CA 90278

**NORTHROP GRUMMAN**

**Raytheon**



**Engineering & Manufacturing Development (EMD) Phase  
Acquisition & Operations Contract**

CAGE NO. 11982

**VIIRS Ice Surface Temperature  
Algorithm Theoretical Basis Document ATBD (ref Y2405)**

**Document Date: 12/22/2010**

**Document Number: D43761  
Revision: B**

**Point of Contact:** Justin Ip, Algorithms & Cal/Val

**ELECTRONIC APPROVAL SIGNATURES:**

\_\_\_\_\_  
Roy Tsugawa, Algorithms & Cal/Val Lead

\_\_\_\_\_  
\_\_\_\_\_

Prepared by  
**Northrop Grumman Aerospace Systems**  
One Space Park  
Redondo Beach, CA 90278

Prepared for  
**Department of the Air Force**  
NPOESS Integrated Program Office  
C/O SMC/CIK  
2420 Vela Way, Suite 1467-A8  
Los Angeles AFB, CA 90245-4659

Under  
**Contract No. F04701-02-C-0502**

COMMERCE DESTINATION CONTROL STATEMENT

The export of these commodities, technology or software are subject to the U.S. Export Laws and Regulations in accordance with the Export Administration Regulations. Diversion contrary to U.S. law is prohibited.

Northrop Grumman Aerospace Systems  
 One Space Park  
 Redondo Beach, CA 90278



**Revision/Change Record**

Document Number D43761

Revision	Document Date	Revision/Change Description	Pages Affected
---	1/26/2007	Initial PCIM Release to bring document into Matrix Accountability. Reference original document number: Y2405 delivered in 2005	All
A	07/31/2008	Replacement of ITAR marking with Commerce Distribution statement	All
B	12/22/2010	<p>Ice Surface Temperature ATBD Corrections for Consistency with EDRPR Update to Revision B (ALG00001649)</p> <p>Updated cover page to refer to Northrop Grumman Aerospace Systems</p> <p>Updated glossary with acroynms for ASF, IP and VCM</p> <p>Updated document references and reference numbers in section 1.3 and A.1.3</p> <p>Updated Section 1.4 Revisions with revision notes</p> <p>Updated Y document numbers with D numbers where appropriate</p> <p>Updated Section 3.5.2 Programming and Procedural Considerations to refer to the VIIRS Ice Surface Temperature EDR OADm EDRIR and EDRPR documents</p> <p>Updated Section 3.5.4 Quality Assessment and Diagnostics. Eliminated detailed quality flag format tables that are more appropriately described in the OAD.</p> <p>Updated Section A.1.4 Revisions with description of the revision for the ST IP</p> <p>Updated Section A.3.1 Processing Outline. Eliminated obsolete architecture flow diagram and replaced it with descriptive text and a reference to the Ice Quality/STIP OAD</p> <p>Updated Table A-2 with correct source and references</p> <p>Updated Section A3.5.3 Quality Assessment and Diagnostics to delete TBD. Provided reference to the VIIRS Ice Quality/STIP OAD. Deleted detailed format table of ST IP quality flags which are described in the OAD.</p>	<p>Cover page</p> <p>p, xiii</p> <p>p. 1-2</p> <p>p. 2</p> <p>All</p> <p>p21</p> <p>p 21-24</p> <p>p, 31</p> <p>p. 34-36</p> <p>p. 37</p> <p>p, 45-46</p>



# **ICE SURFACE TEMPERATURE VISIBLE/INFRARED IMAGER/RADIOMETER SUITE ALGORITHM THEORETICAL BASIS DOCUMENT**

**SDRL No. 151-3  
RAYTHEON COMPANY  
INTELLIGENCE AND INFORMATION Systems (IIS)  
NPOESS Program  
Aurora, Colorado  
Copyright © 2004  
Raytheon Company  
Unpublished Work  
ALL RIGHTS RESERVED**

This documentation/technical data was developed pursuant to Contract Number F04701-02-C-0502 with the US Government under subcontract number 47974DGM2S. The US Government's rights in and to this copyrighted data are as specified in DFAR 252.227-7014, which was made part of the above contract.

IAW DFARS 252.227-7036, Raytheon hereby declares that, to the best of its knowledge and belief, the technical data delivered under Subcontract No. 47974DGM2S is complete, accurate, and complies with all requirements of the Subcontract.

TITLE: ICE SURFACE TEMPERATURE VISIBLE/INFRARED IMAGER/RADIOMETER  
SUITE ALGORITHM THEORETICAL BASIS DOCUMENT

APPROVAL SIGNATURES:

\_\_\_\_\_ 30 March, 2004  
Richard J Sikorski                      Date  
ST Module Lead

\_\_\_\_\_ 30 March, 2004  
Kenneth A St Jensen                      Date  
Task Lead

<b>Northrop Grumman Space &amp; Mission Systems Corp.</b>  <b>Space Technology</b>  <b>One Space Park</b> <b>Redondo Beach, CA 90278</b>			
<b>Revision/Change Record</b>			<b>For Document No.</b> Y2405
Revision	Document Date	Revision/Change Description	Pages Affected
V5r5	15 January 2005	SPCR ALG00000690 Update the IST EDR quality flag table according to the EDRPR v1.7, A2	p. 2, 20, 21, 22, 23
V5r4	30 July 2004	SPCR ALG00000475 Update inconsistency with the IST EDR and ST IP science codes, I/O and LUT descriptions, and ST IP algorithm and regression equation	All pages
V5r3	20 March 2004	SPCR ALG00000024 Update inconsistency in revision number	Title Page, Page 1

### Revision/Change History

Revision	Document Date	Revision/Change Description	Pages Affected
V5r5	15 January, 2005	Update the IST EDR quality flag table according to the EDRPR v1.7 A2	All
V5r4	30 July, 2004	Correct errors and inconsistency with the IST EDR and ST IP science codes, revise the ST IP regression equation, and update quality flags	All
V5r3	30 March, 2004	Appendix revisions per VIIRS Continuance	All

RAYTHEON Technical Services Co, LLC  
ITSS  
1616 McCormick Dr  
Upper Marlboro, MD 20774

## TABLE OF CONTENTS

<b>GLOSSARY OF ACRONYMS .....</b>	<b>ix</b>
<b>ABSTRACT .....</b>	<b>x</b>
<b>1.0 INTRODUCTION .....</b>	<b>1</b>
1.1 PURPOSE .....	1
1.2 SCOPE .....	1
1.3 VIIRS DOCUMENTS.....	1
1.4 REVISIONS .....	2
<b>2.0 EXPERIMENT OVERVIEW .....</b>	<b>3</b>
2.1 OBJECTIVES OF ICE SURFACE TEMPERATURE RETRIEVALS .....	3
2.2 INSTRUMENT CHARACTERISTICS.....	3
2.3 ICE SURFACE TEMPERATURE RETRIEVAL STRATEGY.....	4
<b>3.0 ALGORITHM DESCRIPTION .....</b>	<b>6</b>
3.1 PROCESSING OUTLINE.....	6
3.2 ALGORITHM INPUT .....	7
3.2.1 VIIRS Data.....	7
3.2.2 Non-VIIRS Data .....	8
3.3 THEORETICAL DESCRIPTION OF ICE SURFACE TEMPERATURE RETRIEVAL.....	8
3.3.1 Physics of the Problem .....	8
3.3.2 Mathematical Description of the Algorithm.....	13
3.3.2.1 Split Window Regression.....	13
3.3.2.2 Calibrated Top Of Atmosphere (TOA) Brightness Temperatures .....	13
3.3.3 Archived Algorithm Output.....	14
3.3.4 Variance and Uncertainty Estimate.....	14
3.4 ALGORITHM SENSITIVITY STUDIES.....	18
3.4.1 Ice Water Mixing .....	18
3.5 PRACTICAL CONSIDERATIONS.....	19
3.5.1 Numerical Computation Considerations.....	19
3.5.2 Programming and Procedural Considerations .....	20
3.5.3 Configuration of Retrievals.....	20
3.5.4 Quality Assessment and Diagnostics.....	20
3.5.5 Exception Handling .....	20
3.6 ALGORITHM VALIDATION.....	21
3.6.1 Pre-Launch Validation.....	21
3.6.2 Post-Launch Validation .....	21
<b>4.0 ASSUMPTIONS AND LIMITATIONS.....</b>	<b>22</b>
<b>5.0 REFERENCES.....</b>	<b>23</b>
<b>APPENDIX A: SURFACE TEMPERATURE INTERMEDIATE PRODUCT .....</b>	<b>24</b>

<b>A.1.0</b>	<b>INTRODUCTION .....</b>	<b>24</b>
A.1.1	PURPOSE.....	24
A.1.2	SCOPE.....	24
A.1.3	VIIRS DOCUMENTS .....	25
A.1.4	REVISIONS.....	25
<b>A.2.0</b>	<b>OVERVIEW.....</b>	<b>26</b>
A.2.1	OBJECTIVES OF SURFACE TEMPERATURE RETRIEVAL AT IMAGERY RESOLUTION .....	26
A.2.2	INSTRUMENT CHARACTERISTICS .....	26
A.2.3	SURFACE TEMPERATURE IP RETRIEVAL STRATEGY.....	27
<b>A.3.0</b>	<b>ALGORITHM DESCRIPTION.....</b>	<b>28</b>
A.3.1	PROCESSING OUTLINE .....	28
A.3.2.1	VIIRS Data.....	29
A.3.2.2	Non-VIIRS Data .....	30
A.3.3	THEORETICAL DESCRIPTION OF SURFACE TEMPERATURE IP RETRIEVAL.....	31
A.3.3.1	Physics of the Problem .....	31
A.3.3.2	Mathematical Description of the Algorithm.....	31
A.3.3.2.1	Split Window Regression .....	31
A.3.3.2.2	Calibrated TOA Brightness Temperatures .....	31
A.3.3.2.3	Fusion with Imagery Resolution Band.....	32
A.3.3.3	Single Band Fallback .....	34
A.3.3.4	Archived Algorithm Output.....	34
A.3.3.5	Variance and Uncertainty Estimate.....	34
A.3.4	ALGORITHM SENSITIVITY STUDIES .....	36
A.3.5	PRACTICAL CONSIDERATIONS .....	37
A.3.5.1	Numerical Computation Considerations.....	37
A.3.5.2	Programming and Procedural Considerations .....	37
A.3.5.3	Quality Assessment and Diagnostics.....	37
A.3.5.4	Exception Handling.....	38
A.3.6	ALGORITHM VALIDATION.....	38
A.3.6.1	Pre-Launch Validation.....	38
A.3.6.2	Post-Launch Validation .....	38
<b>A.4.0</b>	<b>ASSUMPTIONS AND LIMITATIONS .....</b>	<b>39</b>
<b>A.5.0</b>	<b>REFERENCES .....</b>	<b>40</b>

## LIST OF FIGURES

Figure 1. IR radiance at the satellite for five atmospheres simulated by MODTRAN. ....	4
Figure 2. Atmospheric transmittance for five atmospheres. ....	5
Figure 3. IST high level flowchart: regression method. ....	6
Figure 4. The relationship between temperature deficits at 10.8 $\mu\text{m}$ band and at 12 $\mu\text{m}$ band. ....	12
Figure 5. The relationship between IST and brightness temperature at the 12 $\mu\text{m}$ band. ....	12
Figure 6. Upper panel: Global IST field. Middle panel: The retrieved IST values. Lower panel: The difference between the IST values. ....	15
Figure 7. IST precision, accuracy, and uncertainty derived from the split window algorithms. ....	16
Figure 8. IST precision, accuracy, and uncertainty derived from the single band algorithms. ....	17
Figure 9. Left panel is the surface temperature derived using IST algorithm, middle is derived from the SST algorithm, and the right is the difference. ....	18
Figure 10. Left panel is the surface temperature derived using the IST algorithm, middle is derived from the SST algorithm, and the right is the difference. ....	19
Figure A-1. Spectral response functions for VIIRS bands M15 (10.8 $\mu\text{m}$ ), I5 (11.5 $\mu\text{m}$ ), and M16 (12.0 $\mu\text{m}$ ). ....	27
Figure A-1. NEdT performance estimates for bands I5, M15, and M16 .....	36

**LIST OF TABLES**

Table 1. VIIRS data for the IST EDR .....7  
Table A-1. VIIRS bands used for Surface Temperature IP .....26  
Table A-2. VIIRS data for the Surface Temperature IP .....29

## GLOSSARY OF ACRONYMS

ARP	Application-Related Product
ASF	Algorithm Support Function
ATBD	Algorithm Theoretical Basis Document
ATSR	Along Track Scanning Radiometer
AVHRR	Advanced Very High Resolution Radiometer
ECMWF	European Center for Medium-Range Weather Forecast
EDR	Environment Data Record
IP	Intermediate Product
IR	Infrared
IST	Ice Surface Temperature
LUT	Look Up Table
LWIR	Longwave Infrared
MODIS	Moderate Resolution Imaging Spectroradiometer
MODTRAN	Moderate Resolution Atmospheric Radiance and Transmittance Model
MOSART	Moderate Spectral Atmosphere Radiance and Transmittance
NCEP	National Centers for Environment Prediction
NEdT	Noise Equivalent Delta Temperature
NPOESS	National Polar-orbiting Operational Environmental Satellite System
P <sup>3</sup> I	Pre-Planned Product Improvements
RMS	Root Mean Square
SBRS	Santa Barbara Remote Sensing
SDR	Sensor Data Record
SST	Sea Surface Temperature
VCM	VIIRS Cloud Mask
VIIRS	Visible/Infrared Imager/Radiometer Suite

## ABSTRACT

This is the Algorithm Theoretical Basis Document (ATBD) for Ice Surface Temperature (IST) retrieval from infrared (IR) signals received by the National Polar-orbiting Operational Environmental Satellite System (NPOESS) Visible/Infrared Imager/Radiometer Suite (VIIRS).

This document describes the theoretical basis and development process of the IST algorithm being developed by the NPOESS algorithm team. The VIIRS IST algorithm is based on a water vapor correction method. It utilizes brightness temperatures from two of the VIIRS Longwave Infrared channels (M15 at 10.8  $\mu\text{m}$  and M16 at 12.0  $\mu\text{m}$ ). The major error sources for IST retrievals are the atmospheric correction and VIIRS sensor performance. There are a number of difficulties in evaluating the accuracy of satellite estimates of IST. These include the difficulty in distinguishing the snow/ice surface from clouds, and the lack of high-quality in situ data. Currently, the uncertainty of IST measurements derived from the Advanced Very High Resolution Radiometer (AVHRR) is about 1.5 K.

Calibration and algorithm validation are the two keys to ensure the performance of the algorithm. Both pre-launch and post-launch activities are discussed in this document. Our simulations show that the VIIRS IST split window algorithm meets the VIIRS IST uncertainty requirement. The validation of the VIIRS IST algorithm will strongly depend on the establishment of the matchup database.

The major constraints for the surface temperature algorithm are instrument band selection; instrument Noise Equivalent Delta Temperature (NE $\Delta$ T) for each band; instrument calibration; and the availability and quality of the surface calibration/validation observations.

## 1.0 INTRODUCTION

### 1.1 PURPOSE

This document describes the theoretical basis and development process of the IST algorithms, for retrieval of the VIIRS IST EDR and the VIIRS Surface Temperature Intermediate Product (ST IP).

### 1.2 SCOPE

The IST algorithms described in this ATBD will be used to routinely retrieve IST from VIIRS. Section 2 of this ATBD provides an overview of the IST algorithm. A description of the algorithm and the development process are presented in Section 3. Section 3 also addresses the error budget, algorithm sensitivity, and validation. Constraints, assumptions, and limitations are discussed in Section 4, and Section 5 presents all citation references in this document. Appendix A is the ST IP ATBD.

### 1.3 VIIRS DOCUMENTS

This document contains references to other VIIRS documents, document numbers are given in italicized brackets:

*[SY15-0007]* - NPOESS System Specification

*[D36385]* - EDR Interdependency Report

*[D37005]* - EDR Production Report

*[D43766 (Y2412)]* - VIIRS Cloud Mask ATBD

*[D36816]* - Operational Algorithm Description Document for VIIRS Cloud Mask Intermediate Product

*[D43311 (Y2386)]* VIIRS Sea Surface Temperature ATBD

*[D36815]* - Operational Algorithm Description Document for Sea Surface Temperature

*[Y2469]* VIIRS Context Level Software Architecture document

*[D43313 (Y2388)]* - VIIRS Aerosol Properties ATBD

*[D39292]* - Operational Algorithm Description Document for VIIRS Aerosol Products IP/EDR

*[Y2479]* - VIIRS Build SDR Module Level Software Architecture

*[Y2473]* - VIIRS Surface Temperature Module Level Software Architecture document

*[D43777 (Y3261)]* - VIIRS Radiometric Calibration ATBD

*[D41063]* - VIIRS Sea Ice Characterization ATBD

[D42821] - Operational Algorithm Description Document for VIIRS Sea Ice Quality Intermediate Product (IP) and Surface Temperature IP

[D42820] - Operational Algorithm Description Document for VIIRS Sea Ice Concentration Intermediate Product

[D39141] - Operational Algorithm Description Document for VIIRS Ice Surface Temperature EDR

## 1.4 REVISIONS

This Revision B document dated December 22, 2010, corrects a statement regarding production of the product for probably cloudy pixels. The previous version failed to state that the IST would be also be produced for probably cloudy pixels. Also, Table 2 which provided a detailed format description of the quality flags has been updated for consistency with VIIRS Ice Surface Temperature Operational Algorithm Description Document (D39141 Rev A) and the Common Data Format Control Book (CDFCB D34862-04-3) and the NPP Environmental Data Record Production Report (D37005 Rev F) . The fifth revision of this document, dated January 2005. The third version of this document was delivered by ITSS per SDRL 151-3 under subcontract from NGST to modify the ST IP science code. Substantial contributions to prior versions of this document were made by Yimin Ji and Philip E. Ardanuy.

## 2.0 EXPERIMENT OVERVIEW

### 2.1 OBJECTIVES OF ICE SURFACE TEMPERATURE RETRIEVALS

Ice Surface Temperature is a crucial measure of the Arctic climate. It is a good indicator of the energy balance at the ice surface. The energy exchange between atmosphere and ice layer influences the global climate by controlling the mass balance. A long-term data set of IST can be used to detect and understand the greenhouse effect and climate changes in the polar region. For years the collection of IST has relied on *in situ* measurement from ships, manned ice camps and drifting buoys. The data coverage and our knowledge of the Arctic IST remains poor compared with the other part of the earth's surface. When sufficiently calibrated, satellite retrieval of IST provides this coverage.

Although much effort has gone into evaluating the accuracy of satellite measurement of sea surface temperature, there has been no comparable effort for IST. This is due to the considerably greater difficulty in distinguishing the ice surface from clouds and the lack of sufficient high quality *in situ* data. The current Root Mean Squared (RMS) error of satellite retrieved IST is about 1 to 3 K (Yu *et al.*, 1995; Key *et al.*, 1994). However, the IST has not been retrieved operationally. In general the moisture is lower in the polar atmospheres, although it is significant in many cases. The IST retrieval methods are split-window statistical methods. Due to the dry air over polar regions, it is often possible to retrieve IST from only one channel within these regions.

The overall scientific objective of the VIIRS IST retrievals is to provide improved measures of global and regional IST fields. The VIIRS IST EDR requires a 0.5 K measurement uncertainty. The requirements are met, provided accurate cloud/ice discrimination is available.

### 2.2 INSTRUMENT CHARACTERISTICS

The VIIRS sensor design is based on the NPOESS sensor requirements and EDR thresholds and objectives. VIIRS bands in the Longwave Infrared (LWIR) were placed to optimize their use for Sea Surface Temperature (SST). Bands in the LWIR are usually located near the maximum earth radiance. The influence of ozone and other atmospheric absorbers must be avoided. Figure 1 shows the Moderate Resolution Atmospheric Radiance and Transmittance Model (MODTRAN) simulated radiance at satellite height for the thermal infrared spectrum. There are a total of five standard atmospheres. There are two regions suitable for LWIR band selection: 8-9  $\mu\text{m}$  and 10-13  $\mu\text{m}$ . VIIRS LWIR bands are located in these two regions. Bands in the far-infrared also need to be placed where the atmosphere is most transparent. Figure 2 shows the MODTRAN simulated atmospheric transmittance for five standard atmospheres. It shows that the 10-13  $\mu\text{m}$  region is one of the most transparent atmosphere windows for arctic atmospheres.

## 2.3 ICE SURFACE TEMPERATURE RETRIEVAL STRATEGY

A Cloud Mask, a Land/Ocean Mask, and a Snow/Ice mask are necessary to eliminate cloud contaminated pixels, land pixels, and ocean pixels. The IST algorithms are run under confident clear, probably clear, and probably cloudy conditions. The brightness temperatures are calculated for the two bands for all suitable pixels within a region.

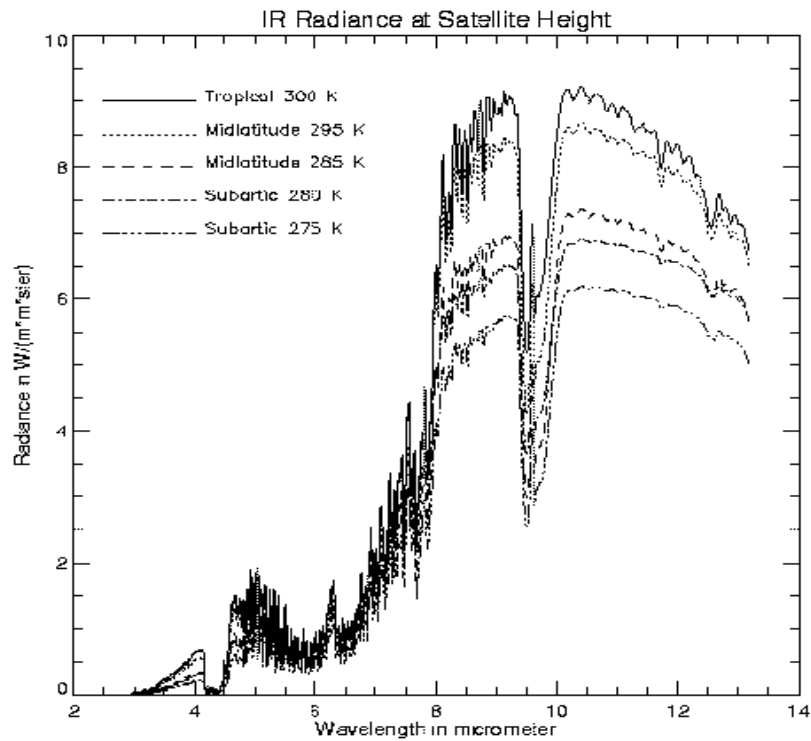


**Figure 1. IR radiance at the satellite for five atmospheres simulated by MODTRAN.**

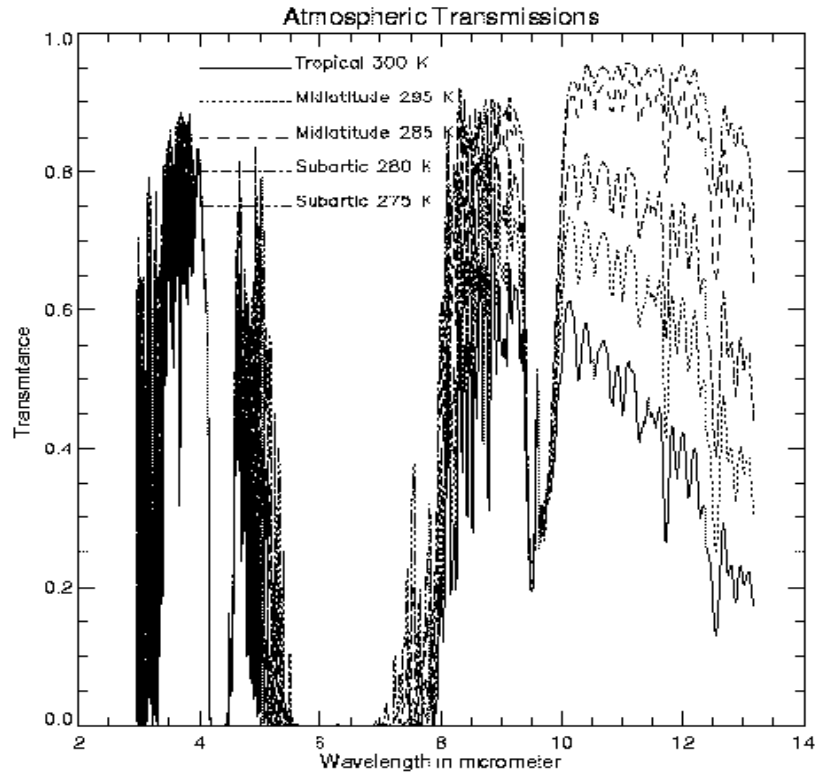


**Figure 2. Atmospheric transmittance for five atmospheres.**

### 3.0 ALGORITHM DESCRIPTION

#### 3.1 PROCESSING OUTLINE

The VIIRS IST retrieval uses an Along Track Scanning Radiometer (ATSR) like regression method. Regression methods are initially assisted by the establishment of ancillary data and radiative transfer models. The coefficients of regression equations are obtained from simulation processes. Figure 3 depicts the processing concept for statistical IST retrieval.

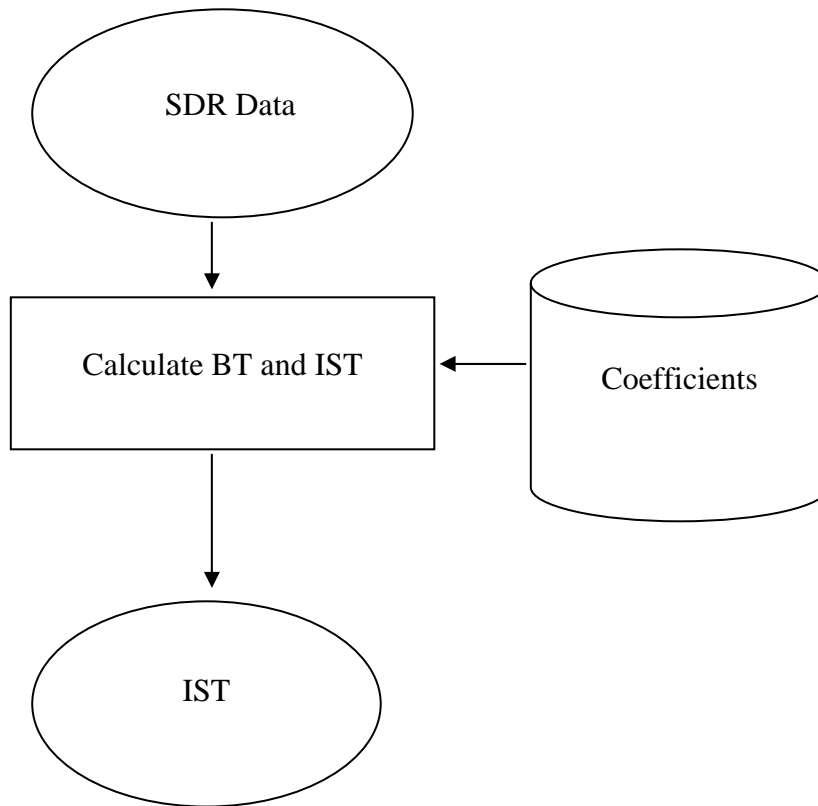


**Figure 3. IST high level flowchart: regression method.**

## 3.2 ALGORITHM INPUT

### 3.2.1 VIIRS Data

The VIIRS data presented in Table 1 are required input to the algorithm processing code.

**Table 1. VIIRS data for the IST EDR**

<b>Input Data</b>	<b>Source of Data</b>
Instrument (Band) Quality	VIIRS Sensor Data Record (SDR)
Brightness Temperature (M15 and M16)	VIIRS SDRs
Solar/Sensor Angles	VIIRS SDRs
Aerosol Optical Thickness (AOT)	Aerosol Optical Thickness IP
Cloud Mask	Cloud Mask IP
Ice Fraction	VIIRS Ice Concentration IP

#### ***Instrument (Band) Quality***

The VIIRS EV\_750M SDR will contain band M15 and M16 quality flags at moderate pixel resolution. Pixels with bad quality will not be processed. A poor quality flag will be set for these pixels.

#### ***Brightness Temperatures***

Brightness temperatures for the M15 and M16 bands are obtained from the VIIRS EV\_750M SDR.

#### ***Solar / Sensor Angles***

The sensor zenith angle is used in the split window algorithm and is part of the SDR.

#### ***Aerosol Optical Thickness***

Aerosol optical thickness is used for performance exclusion for slant path AOT > 1.0.

#### ***Cloud Mask***

The VIIRS cloud mask [D43766] is expected to derive a status of confident clear / probably clear / probably cloudy / confident cloudy for each pixel, building on Moderate Resolution Imaging Spectroradiometer (MODIS) cloud mask heritage (Ackerman *et al.*,

1997). Pixels classified as “confident cloudy” will be excluded from further processing. Pixels classified as “probably clear” or as “confident clear” will be processed and flagged for degraded quality. This determination must depend on an assessment of the cloud mask performance, particularly over snow and ice surfaces.

### **Ice Concentration**

The VIIRS Ice Concentration IP is an imagery resolution product derived by the Ice Concentration module [D41063; D42820]. It provides the ice fraction within the moderate resolution pixels after aggregation from the imagery resolution pixels.

#### **3.2.2 Non-VIIRS Data**

The algorithm requires no input data from outside the VIIRS system.

### **3.3 THEORETICAL DESCRIPTION OF ICE SURFACE TEMPERATURE RETRIEVAL**

#### **3.3.1 Physics of the Problem**

In clear sky conditions, the outgoing infrared spectral radiance at the top of atmosphere can be represented by:

$$L(\lambda, \mu) = \tau(\lambda, \mu)\varepsilon(\lambda, \mu)B(\lambda, T_s) + L_a(\lambda, \mu) + L_s(\lambda, \mu, \mu_0, \varphi_0) + L_d(\lambda, \mu, \mu_0, \varphi_0) + L_r(\lambda, \mu, \mu_0, \varphi_0) \quad (1)$$

Where  $\tau$  is the transmissivity,  $\varepsilon$  the surface spectral emissivity,  $B$  the Plank function,  $L_a$  the thermal path radiance,  $L_s$  the path radiance resulting from scattering of solar radiation.  $L_d$  is the solar radiance and  $L_r$  the solar diffuse radiation and atmospheric thermal radiation reflected by the surface.  $\lambda$  is the wavelength.  $\mu = \cos(\theta)$ ,  $\mu_0 = \cos(\psi)$ , where  $\theta$  is the satellite zenith angle,  $\psi$  the solar zenith angle.  $\varphi_0$  is azimuth angle.

The wavelength is the wavelength center of a narrow interval because there is no way to measure the exact monochromatic signal as a continuous function of wavelength by satellite sensors. Equation 1 can be used in the 3-14  $\mu m$  range. It requires complete calculations of the atmospheric radiative transfer to determine the values of all terms on the right side. This equation has been used in many atmospheric radiation models including the Low-resolution Transmission Model (LOWTRAN) (Kneizys *et al.*, 1988), MODTRAN (Berk *et al.*, 1987), and the Moderate Spectral Atmosphere Radiance and Transmittance (MOSART) (Cornette *et al.*, 1994).

The satellite infrared radiance can be corrected for atmospheric absorption in the water vapor bands by utilizing a split window technique. In the following discussion, we outline a theoretical basis for the split window method.

For LWIR bands,  $L_d$ ,  $L_s$  and  $L_r$  are negligible. Therefore, only the first two terms on the right side of the above equation are important. In this case, if we ignore the change of emissivity over the ocean, the radiance error introduced by the atmosphere  $\Delta L$  can be represented by:

$$\begin{aligned}\Delta L &= B(\lambda, T_s) - L(\lambda, \mu) = B(\lambda, T_s) - \tau(\lambda, \mu)B(\lambda, T_s) - L_a(\lambda, \mu) \\ &= - \int_1^{\tau(\lambda, \mu)} B(\lambda, T_s) d\tau(\lambda, \mu, p) + \int_1^{\tau(\lambda, \mu)} B(\lambda, T_p) d\tau(\lambda, \mu, p) \\ &= - \int_1^{\tau(\lambda, \mu)} (B(\lambda, T_s) - B(\lambda, T_p)) d\tau(\lambda, \mu, p)\end{aligned}\quad (2)$$

From the Planck function we find:

$$\Delta L = \frac{\partial B}{\partial T} \Delta T = \frac{\partial B}{\partial T} (T_s - T_\lambda) \quad (3)$$

For an optically thin gas the following approximations can be made:

$$d\tau = d(e^{-k_\lambda l}) = -k_\lambda dl \quad (4)$$

Where  $k_\lambda$  is the absorption coefficient and  $l$  is the optical path-length. If we assume that the Planck function is adequately represented by a first order Taylor series expansion in each channel window, then:

$$B(\lambda, T_s) - B(\lambda, T_p) = \left. \frac{\partial B(\lambda, T_p)}{\partial T} \right|_{T_s} (T_p - T_s) \quad (5)$$

Substituting Equations 3, 4, 5 into Equation 2, we obtain:

$$T_s - T_\lambda = k_\lambda \int_1^{\tau} (T_s - T_p) dl \quad (6)$$

Therefore, if we pick two spectral regions of the atmosphere, we have two linear equations with different  $k_\lambda$  to solve simultaneously.

For example, if we consider two channels as  $\lambda=1$  and  $\lambda=2$ , then we get:

$$T_s - T_1 = -(T_s - T_2)k_1/k_2 \quad (7)$$

Figure 4 shows the relationship between  $T_s - T_{11}$  and  $T_s - T_{12}$  from MODTRAN simulations. The brightness temperature at the 10.8  $\mu\text{m}$  ( $T_{11}$ ) band is higher than that at the 12  $\mu\text{m}$  band ( $T_{12}$ ). However, the relationship between  $T_s - T_{11}$  and  $T_s - T_{12}$  is rather linear. The maximum difference is only about 3 K.

In general, the ice surface temperature can be represented as:

$$\mathbf{T}_s = \mathbf{C}\mathbf{T}_b \quad (8)$$

The coefficient vector  $\mathbf{C}$ , relating observed brightness temperatures to IST, is determined using regression methods by solving:

$$\mathbf{C} = \mathbf{Y}\mathbf{X}^T(\mathbf{X}\mathbf{X}^T + k\mathbf{I})^{-1} \quad (9)$$

The  $\mathbf{Y}$  matrix contains a large number of training IST, and the  $\mathbf{X}$  matrix contains brightness temperatures from VIIRS LWIR channels. In general, the  $\mathbf{X}$  matrix may include non-linear terms.

Because the atmospheric correction term is small, it is often possible to use only one channel to retrieve IST. Figure 5 shows the relationship between IST and the brightness temperature at the 12  $\mu\text{m}$  band. The relationship is linear.

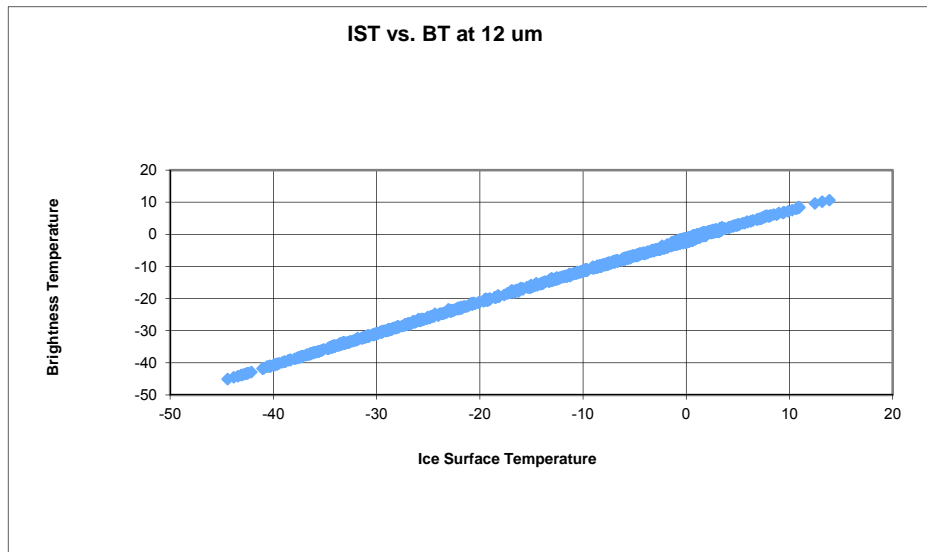
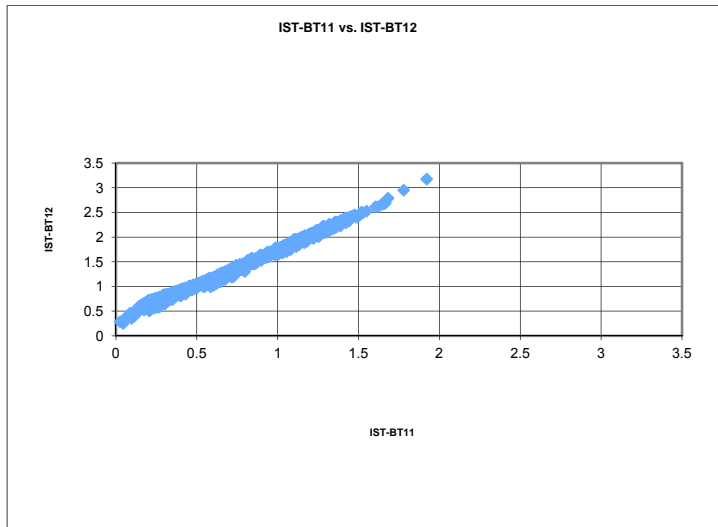


**Figure 4. The relationship between temperature deficits at 10.8  $\mu\text{m}$  band and at 12  $\mu\text{m}$  band.**

**Figure 5. The relationship between IST and brightness temperature at the 12  $\mu\text{m}$  band.**

Currently, the IST uncertainty from the regression algorithm is about 1 to 3 K.

### 3.3.2 Mathematical Description of the Algorithm

#### 3.3.2.1 Split Window Regression

The VIIRS IST algorithm is based on statistical methods. Traditional statistical methods for satellite IST retrieval are linear multi-channel regression methods. The following regression methods are used in the VIIRS IST retrieval:

Split window (10.8 + 12  $\mu\text{m}$  bands, from the Advanced Very High Resolution Radiometer (AVHRR) method, Yu et al., 1995) (VIIRS IST baseline algorithm):

$$\text{IST} = a_0 + a_1 T_{11} + a_2 (T_{11} - T_{12}) + a_3 (\sec(z) - 1) \quad (10)$$

One channel (12  $\mu\text{m}$  band). (VIIRS IST fallback algorithm):

$$\text{IST} = a_0 + a_1 T_{12} + a_2 (\sec(z) - 1) \quad (11)$$

Where  $T_{11}$  and  $T_{12}$  are the VIIRS brightness temperatures at M15 (10.8  $\mu\text{m}$ ) and M16 (12.0  $\mu\text{m}$ ) respectively,  $z$  is the satellite zenith angle, and  $a_0$ ,  $a_1$ ,  $a_2$ ,  $a_3$  are the regression coefficients. Satellite-measured radiance is a function of the atmospheric profiles and surface properties. For the Infrared (IR) window and water vapor channels, the radiance over oceans at the top of the atmosphere is mainly a function of the surface temperature and the temperature and moisture profiles. One can choose a few channels (e.g., 3 channels) for which only the main structures of the temperature and moisture profiles are required to obtain ice surface temperature. The regression coefficients used in the regression equations 10 and 11 are trained against snow covered ice surfaces.

#### 3.3.2.2 Calibrated Top Of Atmosphere (TOA) Brightness Temperatures

The blackbody radiance (R) function is

$$R = 2 h \nu^3 / [c^2 (\exp\{-h\nu/kT\} - 1)] \quad (12)$$

where  $\nu$  is the wavenumber ( $\text{cm}^{-1}$ ),  $h$  is the Planck constant,  $c$  is the speed of light,  $k$  is Boltzman's constant, and  $T$  is the temperature in Kelvin.

Equation 12 can be written as

$$R = c_1 \nu^3 / [c^2 (\exp\{-c_2\nu/T\} - 1)] \quad (13)$$

where  $c_1$  and  $c_2$  are two blackbody constants equal to 0.01191071 and 1.438838 respectively using Centimeter-Gram-Second (CGS) units.

This can be solved for the brightness temperature ( $T$  or  $T_b$ ) to give:

$$T_b = c_2 \nu / \ln(1 / (1 + c_1 \nu^3 / c^2 R)) \quad (14)$$

### 3.3.3 Archived Algorithm Output

VIIRS moderate resolution IST value and the associated quality flags are produced as the IST EDR according to the system specification, and in addition as a imagery resolution Surface Temperature IP (ST IP). (See Appendix A.)

### 3.3.4 Variance and Uncertainty Estimate

IST retrieval uncertainty is determined by many factors, including atmospheric correction, the surface state, and sensor performance. For example, the surface state may be snow cover or melt pond, which have significantly different radiometric properties. And there are a number of error sources in sensor performance, such as sensor noise, calibration error, geolocation, and band-to-band registration.

The data set used to estimate the IST uncertainty and accuracy is a global snapshot of surface temperature at  $2.5^\circ$  by  $2.5^\circ$  resolution supplied by the National Centers for Environment Prediction (NCEP), with matching atmospheric profiles. The data were used to simulate the TOA radiance.

In Figure 6, the upper panel shows the global snapshot of IST at 00Z July 1, 1993 and the middle panel shows the retrieved IST. The lower panel shows the difference. The NEdT values are about 0.1 K for the split window (SBRS baseline sensor specification). The root mean square (RMS) error is about 0.16 K at this noise level without considering any absolute calibration errors. The maximum error is 0.74 K in daytime and 0.46 K in nighttime.

The retrieval error is a function of satellite viewing angles and surface temperature values. In Figure 7, the upper panel shows the IST precision as a function of satellite zenith angle and surface temperature. A 0.2 K absolute calibration error was assumed in this retrieval. The algorithm used is the split window regression method. The precision error is less than 0.3 K for most satellite zenith angles and temperatures. The middle panel shows the IST accuracy error.

The accuracy is generally better than 0.2 K. The lower panel shows the RMS error. The RMS error is less than 0.3 K for higher temperatures and most of the satellite viewing angles. For large zenith angles and lower surface temperatures, the uncertainty is larger, but still less than 0.5 K.

Figure 8 shows the IST precision, accuracy and uncertainty from the single band algorithm. The errors are larger in this algorithm than that in the split window algorithm. But the errors are still less than 0.5 K, except for large satellite viewing angles. These results are relevant for the ST IP at imagery resolution (see Appendix A).

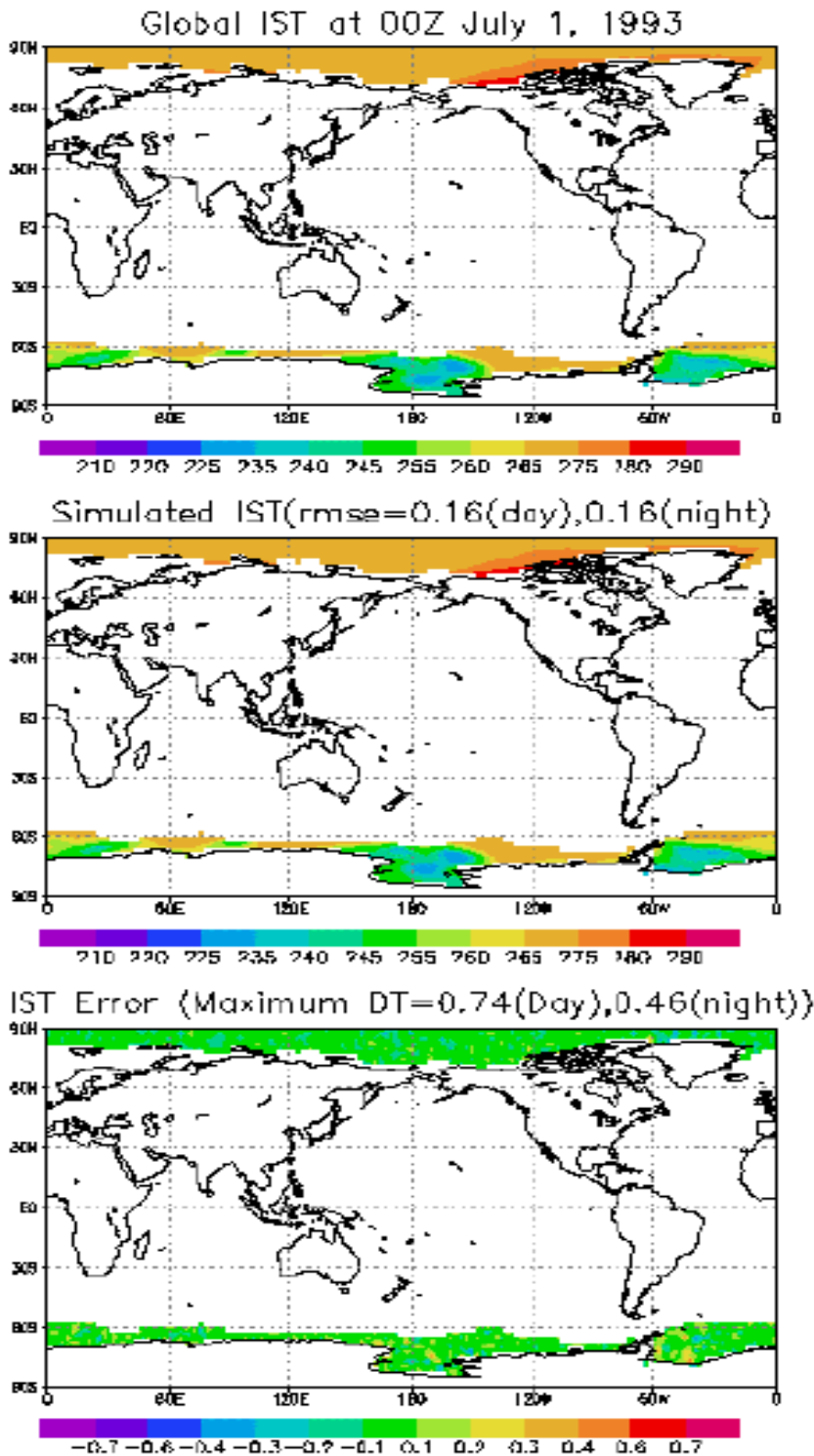
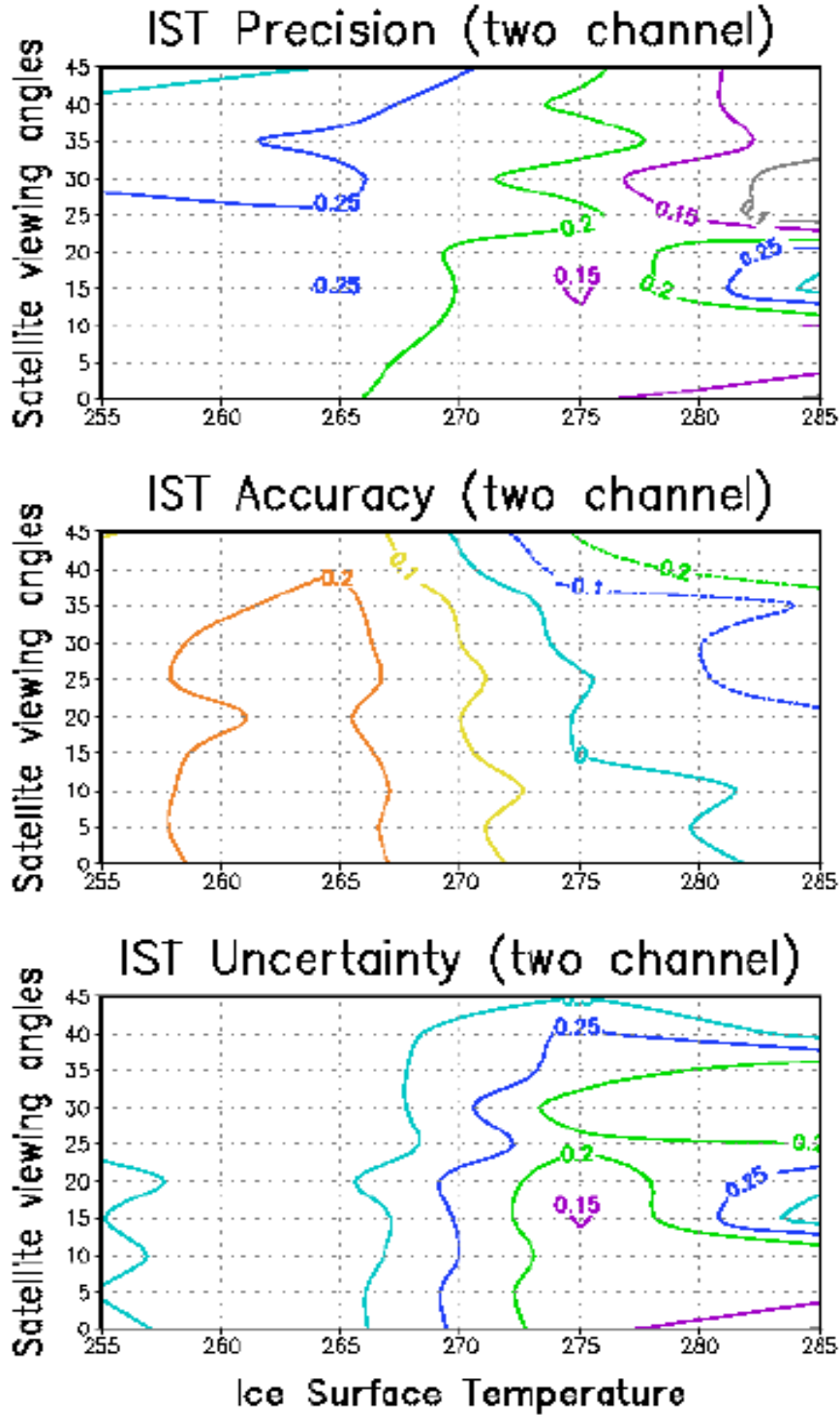
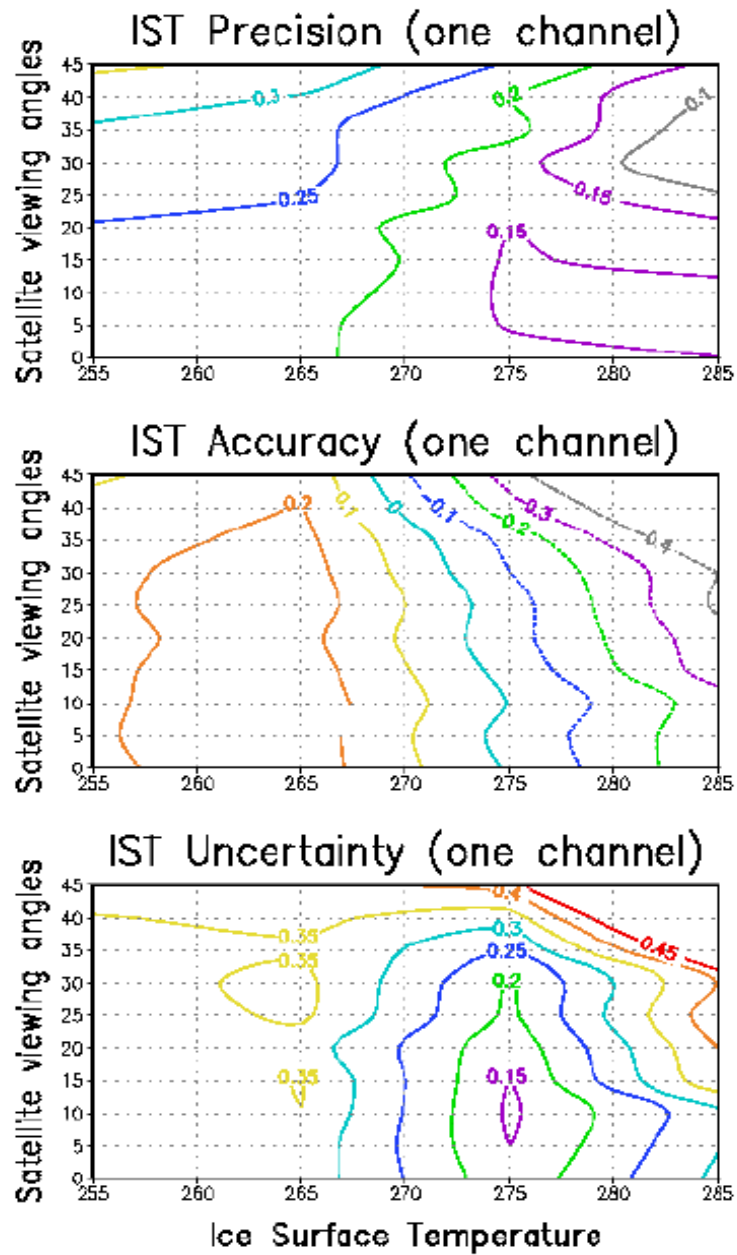


Figure 6. Upper panel: Global IST field. Middle panel: The retrieved IST values. Lower panel: The difference between the IST values.



**Figure 7. IST precision, accuracy, and uncertainty derived from the split window algorithms.**



**Figure 8. IST precision, accuracy, and uncertainty derived from the single band algorithms.**

### 3.4 ALGORITHM SENSITIVITY STUDIES

#### 3.4.1 Ice Water Mixing

Pixels that contain both ice and water are a major geophysical source of error, due to the significantly different radiometric properties of these surfaces. To estimate the error for the mixed region, both the SST algorithm and the IST algorithm were applied to two MODIS Airborne Simulator (MAS) scenes. In Figure 9, the left panel shows the ice surface temperature map, the middle panel shows the map of sea surface temperature and the right panel shows the difference. The difference map indicates that the surface temperatures retrieved using the SST algorithm are generally higher than those derived from the IST algorithm, but the difference is smaller ( $< 0.5$  K) over the ice surface. Over water, the difference can be as high as 1 K. Figure 10 is similar to Figure 9, but for another scene. The result is similar to that of the previous scene.

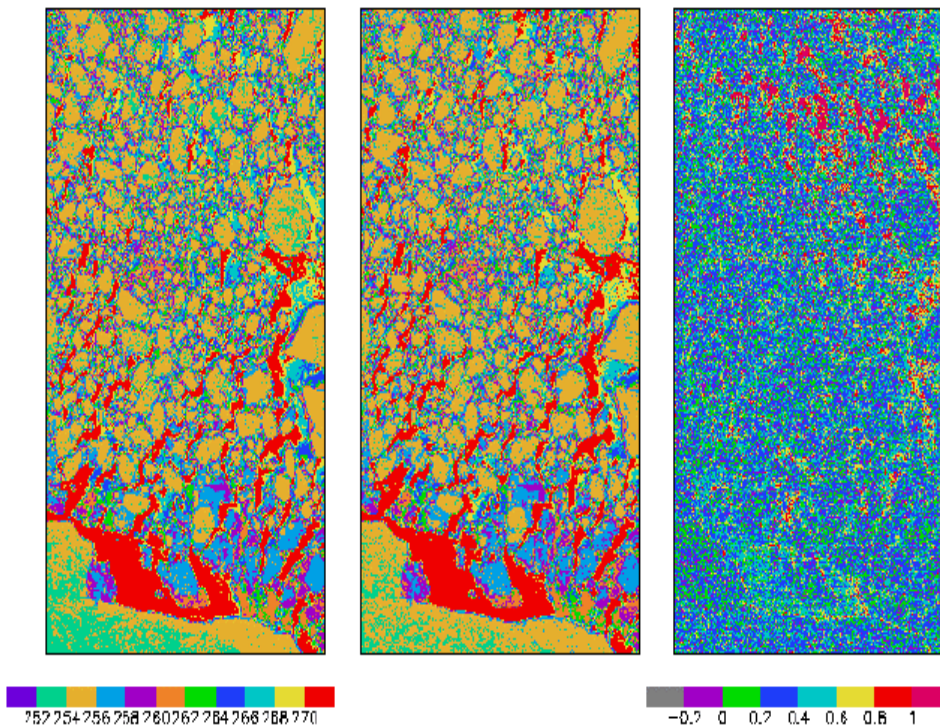


**Figure 9.** Left panel is the surface temperature derived using IST algorithm, middle is derived from the SST algorithm, and the right is the difference.

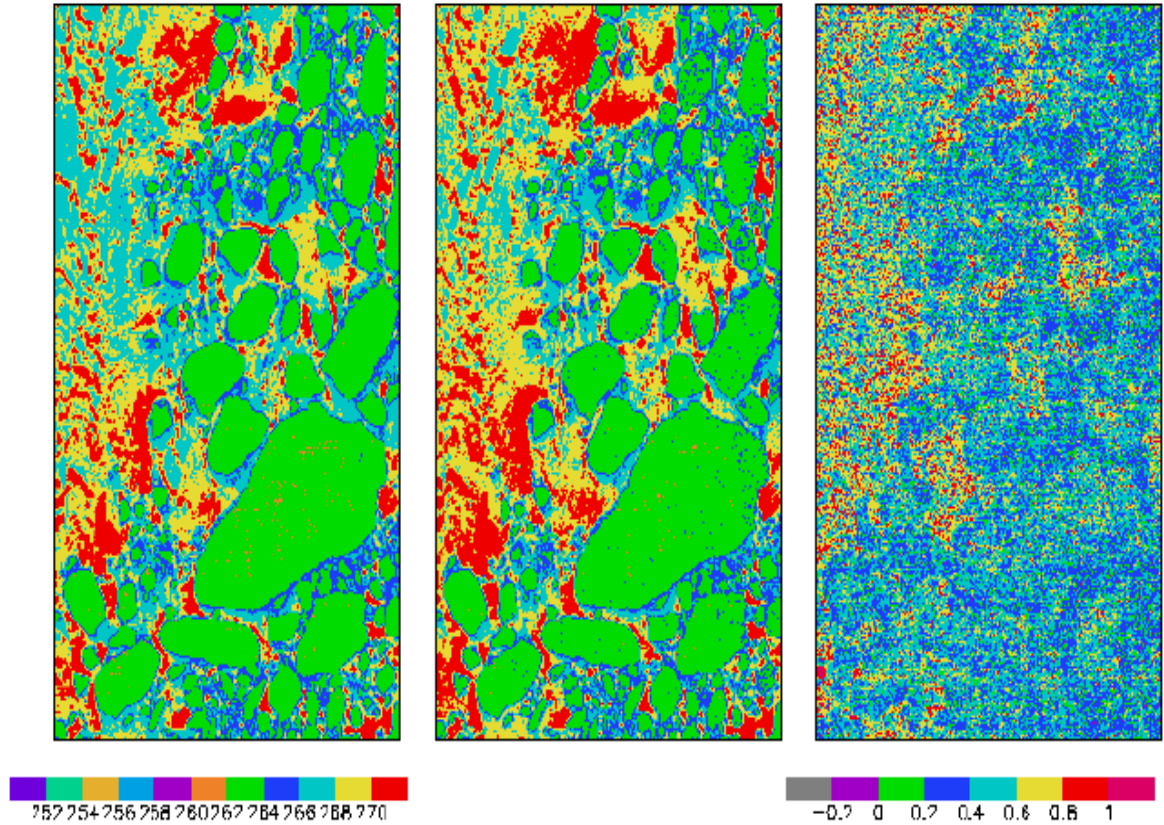


**Figure 10.** Left panel is the surface temperature derived using the IST algorithm, middle is derived from the SST algorithm, and the right is the difference.

### 3.5 PRACTICAL CONSIDERATIONS

#### 3.5.1 Numerical Computation Considerations

In order to retrieve IST within an operational timeframe, statistical algorithms that meet quality requirements have been developed that are much quicker than physical modeling methods. Pre-generated LUTs are used to speed processing yet retain flexibility.

### **3.5.2 Programming and Procedural Considerations**

The simplicity of all the algorithms described in this document translates into very small amounts of code using basic mathematical routines. Computationally intensive processes are performed offline, with results delivered as re-generated LUTs. VIIRS Phase II efforts are largely software-focused, and the methodology for this development work is based on sound and proven principles, as discussed in the VIIRS Algorithm Software Development Plan [Y6635]. The software design and operational implementation relevant to the IST Unit are summarized in the VIIRS Ice Surface Temperature EDR Operational Algorithm Description Document (D39141). These designs are tested at the system level as described in the most recent versions of the VIIRS Software Integration and Test Plan [Y3236], Algorithm Verification and Validation Plan [Y3237], and System Verification and Validation Plan [Y3270]. A summary of the ultimate strategy for operational application of the system of VIIRS algorithms is provided in the VIIRS Operations Concept document [Y2468]. The VIIRS EDR Interdependency Report [D36385] and EDR Production Report [D37005] provide more detail on the specifics of input dependencies and production criteria for the IST EDR and other VIIRS products.

### **3.5.3 Configuration of Retrievals**

Adjustable parameters for the retrieval of the IST products allow post-launch updating of regression coefficients. The flexibility built into the architecture also allows easy implementation of future P<sup>3</sup>I developments.

### **3.5.4 Quality Assessment and Diagnostics**

A number of parameters and indicators are reported in the IST product as retrieval diagnostic quality flags. Quality flags at the pixel level are included for overall retrieval quality, VCM IP cloud confidence, thin cirrus, land/water, day/night, algorithm mode, AOT exclusion, ice fraction. Granule level quality flags include flags for percent of pixels retrieved with high quality, percent of pixels retrieved under exclusion conditions, no ocean in a granule and no land in a granule. A complete description for all IST EDR quality flags and detailed format information is provided in the Operational Algorithm Description Document for the VIIRS Ice Surface Temperature EDR [D39141].

### **3.5.5 Exception Handling**

Confident Cloudy pixels identified by the cloud mask are not processed and flagged. Pixels with bad radiance data are also not processed and flagged.

## **3.6 ALGORITHM VALIDATION**

### **3.6.1 Pre-Launch Validation**

The atmospheric correction algorithm coefficients will be derived pre-launch by radiative transfer modeling to simulate the VIIRS infrared channel measurements. Selected radiosondes from the operational network stations or field campaigns will be used in VIIRS simulations for the development of the atmospheric correction algorithm. Measurements from the operational surface drifting and fixed buoy programs will be used to characterize the surface temperature fields and to validate the atmospheric correction algorithms. The assimilated meteorological fields provided by NCEP and European Center for Medium-Range Weather Forecast (ECMWF) provide a valuable description of the marine atmosphere and surface temperatures. These fields will be used in conjunction with the radiative transfer modeling to simulate the VIIRS measurements, to validate the radiosonde data and to provide direct input to the radiative transfer modeling process.

Measurements from AVHRR, ATSR, and MODIS will be used in the pre-launch phase to study the error characteristics of the IST retrieval.

### **3.6.2 Post-Launch Validation**

The infrared measurements are calibrated by using measurements of cold space and an on-board black body target. This produces radiance in the spectral intervals defined by the system response functions of each channel. These calibrated radiances can be converted to TOA brightness temperatures. To derive IST from the calibrated radiance at TOA, it is necessary to correct the effects of the intervening atmosphere.

The post-launch validation activities are important to test and improve the IST retrieval algorithm. The best retrieval accuracy can be achieved by developing comprehensive in situ data sets that provide adequate sampling of the atmospheric conditions and IST, including long-term studies to reveal sensor drift and the effects of episodic atmospheric changes.

#### 4.0 ASSUMPTIONS AND LIMITATIONS

A limitation of the VIIRS Ice Surface Temperature retrieval is that it can only achieve optimal performance under clear condition. The accuracy of the retrieval is also highly dependent on accurate cloud and ice discriminations.

## 5.0 REFERENCES

- Berk, A., L. S. Bemstein, and D. C. Robertson (1987). MODTRAN: A moderate resolution model for LOWTRAN. Rep. GLTR-89-0122, Burlington, MA: Spectral Sciences, Inc.
- Cornette, W. M., P. K. Acharya, D. C. Robertson, and G. P. Anderson (1994). Moderate spectral atmospheric radiance and transmittance code (MOSART). Rep. R-057-94(11-30), La Jolla, CA: Photon Research Associates, Inc.
- Key, J., J. A. Maslanik, T. Papakyriakou, M. C. Serreze, and A. J. Schweiger (1994). On the validation of satellite-derived sea ice temperature. *Arctic*, 47, 280-287.
- Kneizys, F. X., ., E. P. Shettle, L. W. Abreu, J. H. Chetwynd, G. P. Anderson, W. O. Gallery, J. E. A. Selby, and S. A. Clough (1988). Users guide to LOWTRAN7. Rep. AFGL-TR-88-0177, Bedford, MA: Air Force Geophys. Lab.
- Yu, Y., D. A. Rothrock, and R. W. Lindsay (1995). Accuracy of sea ice temperature derived from the advanced very high resolution radiometer. *J. Geophys. Res.*, 100, 4525-4532.

## APPENDIX A: SURFACE TEMPERATURE INTERMEDIATE PRODUCT

### A.1.0 INTRODUCTION

#### A.1.1 PURPOSE

This appendix provides the theoretical basis for the Surface Temperature IP retrieval from IR signals received by the NPOESS VIIRS. The Surface Temperature IP is produced as required input data for the VIIRS Snow-Ice Module.

The baseline algorithm, based on a water vapor correction method, is adapted from the VIIRS algorithm for the IST EDR retrieval. It will utilize radiances from two of the VIIRS LWIR bands at moderate spatial resolution plus the VIIRS LWIR imagery resolution band, to derive surface temperature at imagery resolution. The fusion of moderate resolution bands with the imagery resolution band is achieved by modeling their spectral response functions. The fallback algorithm uses a single band, and is most effective under dry atmospheres.

Calibration and algorithm validation are the two keys to ensure the performance of the algorithm. Both pre-launch and post-launch activities are discussed in this document. The validation of the VIIRS IST algorithm is discussed in Section A.3.6 of this document.

#### A.1.2 SCOPE

This appendix covers the theoretical basis for the derivation of the Surface Temperature IP, which consists of the surface temperature and associated quality flags at imagery resolution. The purpose and scope are described in Section A.1, while Section A.2 provides an overview of the retrieval objectives. Section A.3 describes the algorithm, its input data, the theoretical background, and some practical considerations. Section A.4 contains the algorithm performance analysis and error budget. Section A.5 contains the pre-launch and post-launch plan for verification and validation. Section A.6 contains assumptions and limitations.

### **A.1.3 VIIRS DOCUMENTS**

This appendix contains references to other VIIRS documents which are given in italicized brackets:

*[SY15-0007]* VIIRS System Specification  
*[PS154640-101]* VIIRS Sensor Specification  
*[D43767 (Y2466)]* VIIRS Imagery ATBD  
*[D43311 (Y2386)]* VIIRS Sea Surface Temperature ATBD  
*[Y2469]* VIIRS Context Level Software Architecture document  
*[Y2471]* - VIIRS Aerosol Module Level Software Architecture  
*[Y2472]* - VIIRS Cloud Module Level Software Architecture  
*[Y2477]* VIIRS Snow/Ice Module Level Software Architecture document  
*[Y2479]* - VIIRS Build SDR Module Level Software Architecture  
*[Y2473]* VIIRS Surface Temperature Module Level Software Architecture document  
*[D43777 (Y3261)]* - VIIRS Radiometric Calibration ATBD  
*[D43313 (Y2388)]* - VIIRS Aerosol Properties ATBD  
*[D39292]* - Operational Algorithm Description Document for VIIRS Aerosol Products IP/EDR  
*[Y3278]* - VIIRS Cloud Module Level Interface Control Document  
*[D41063]* - VIIRS Sea Ice Characterization ATBD  
*[D42821]* - Operational Algorithm Description Document for VIIRS Sea Ice Quality Intermediate Product (IP) and Surface Temperature IP  
*[D42820]* - Operational Algorithm Description Document for VIIRS Sea Ice Concentration Intermediate Product

### **A.1.4 REVISIONS**

This is the first revision of this appendix. This revision provides updates to the references and deletes detail format description tables of the Surface Temperature IP quality flags that are more appropriately described in the Operational Description Document for the VIIRS Sea Ice Quality/Surface Temperature IP [D42821].

The first revision included changes to the ST IP algorithm under the post-CDR VIIRS Continuation work. It is appended to version 5, revision 4 of the VIIRS Ice Surface Temperature ATBD, dated July 2004. The first version of this appendix was appended to version 5 of the VIIRS Ice Surface Temperature ATBD, dated February 2002.

## A.2.0 OVERVIEW

### A.2.1 OBJECTIVES OF SURFACE TEMPERATURE RETRIEVAL AT IMAGERY RESOLUTION

The overall scientific objective of the VIIRS IST retrievals is to provide improved measures of global and regional IST fields. The VIIRS IST EDR requires a global horizontal cell size of 1 km at nadir with 0.5 K measurement uncertainty. The IST algorithm, described earlier in this document, retrieves surface temperature at the moderate resolution of the M15 and M16 bands.

The VIIRS Sea Ice algorithm [D41063] requires surface temperature at imagery resolution as input data. Therefore, the software units that produce the VIIRS ice data products require surface temperature at imagery resolution. The VIIRS IST EDR is produced from moderate resolution data, so is not adequate for this purpose. The VIIRS Snow-Ice Module has therefore placed a requirement on the VIIRS system to provide an additional surface temperature product at imagery resolution.

### A.2.2 INSTRUMENT CHARACTERISTICS

VIIRS moderate resolution bands in the LWIR were placed to optimize their use for SST. Two of these bands (M15 and M16) are used by the split window IST EDR retrieval algorithm. The Surface Temperature IP algorithm will also use these bands for water vapor correction. In addition, the algorithm will use the imagery resolution LWIR band (I5). Band characteristics are indicated in Table A-1. Spectral response functions are illustrated in Figure A-1.

**Table A-1. VIIRS bands used for Surface Temperature IP.**

Band	Center Wavelength (μm)	Band Width <sup>1</sup> (μm)	Nadir resolution (m)	Ttyp	NEdT @ Ttyp (K)
M15	10.76	1.0	750	300 K	0.070
I5	11.45	1.9	375	210 K	1.5
M16	12.01	0.95	750	300 K	0.072

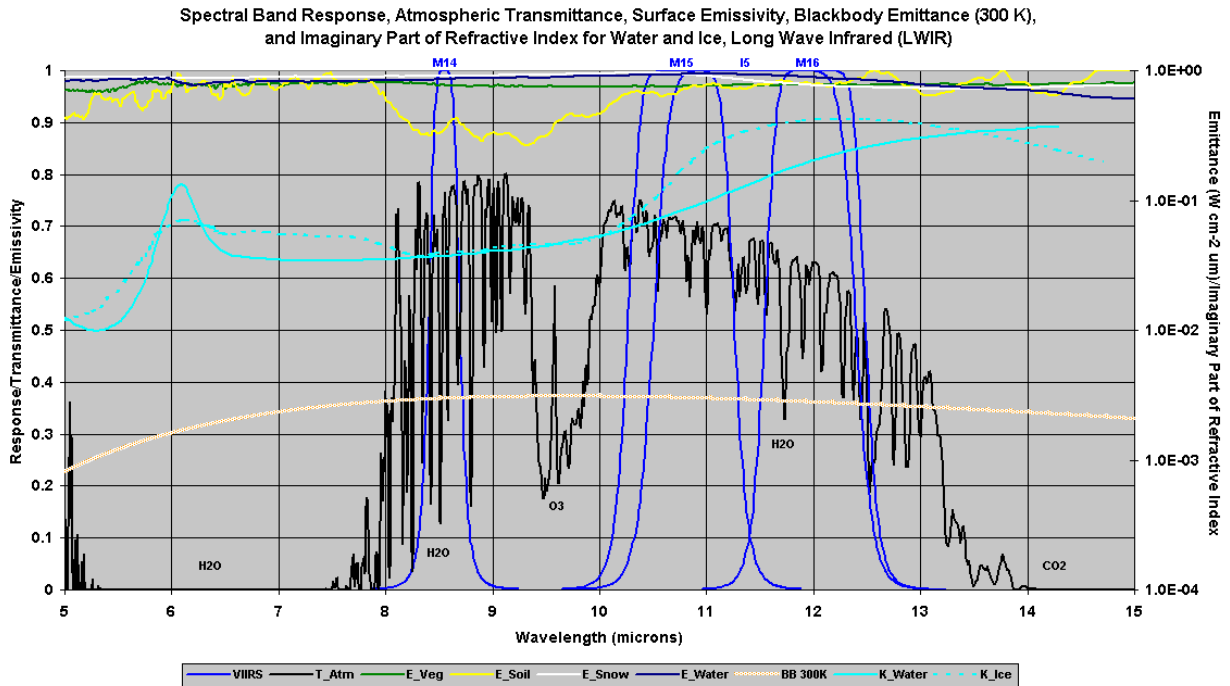


**Figure A-1. Spectral response functions for VIIRS bands M15 (10.8  $\mu\text{m}$ ), I5 (11.5  $\mu\text{m}$ ), and M16 (12.0  $\mu\text{m}$ ).**

### A.2.3 SURFACE TEMPERATURE IP RETRIEVAL STRATEGY

Because the Surface Temperature IP is only used by the ice algorithms, it is only retrieved for regions within the Horizontal Coverage range of the ice ARPs and EDRs. An Ice Quality unit [D42821] in the Snow/Ice module [Y2477] masks pixels outside of the range, de-weights pixels with cloud cover, and writes the results to an Ice Mask IP and an Ice Weights IP. Brightness temperatures for the two moderate resolution bands (M15 and M16) and for the one imagery resolution band (I5) are derived by the Radiometric Calibration unit of the Build-SDR module [D43777].

A LUT (Surface Temperature IP regression coefficients LUT) are generated offline. These contain the regression coefficients required by the baseline 2- band split window and fallback single-band algorithms.

The surface temperature is computed at imagery resolution for all imagery pixels that are not masked, using the brightness temperatures of the I5, M15, and M16 bands. The split window algorithm is used where feasible. If there is bad M15 or M16 data, the single band algorithm is used.

## A.3.0 ALGORITHM DESCRIPTION

### A.3.1 PROCESSING OUTLINE

The Surface Temperature IP algorithm is implemented as a function within the Ice Quality algorithm [D43821]. The Ice Quality algorithm reads brightness temperatures from the VIIRS 750m and 375 m SDRs, VIIRS Cloud Mask IP cloud confidence and quality flags, VIIRS Cloud Optical Properties IP and, 550 nm AOT from the VIIRS AOP IP. The Ice Quality algorithm constructs a mask of quality flags (Ice Quality Flags IP) and quality weights (Ice Quality Weights IP) that are used by the Surface Temperature IP, Sea Ice Concentration IP and Sea Ice Age EDR algorithms. The Surface Temperature IP algorithm uses information from the Ice Quality Flags IP and Ice Quality Weights IP to determine which pixels should be processed as well as assignment of retrieval quality. Regression coefficients periodically generated by an offline Algorithm Support Function (ASF) process and are read as input by the Surface Temperature IP algorithm. The regression coefficients are considered to be trained on snow covered sea ice surfaces since most sea ice is snow covered. The appropriate set of regression coefficients are used by the IST algorithm for the algorithm mode selected (two band IR split window regression algorithm or fallback single band regression algorithm).

For each good quality imagery resolution pixel in the VIIRS granule, the split window regression coefficients are applied to the observed brightness temperature in the I5 band,  $t_i$  and the observed M15-M16 brightness temperature difference for the moderate resolution pixel nearest to the imagery resolution pixel,  $(t_{11\mu m} - t_{12\mu m})$  to determine surface temperature at imagery resolution according to Equation A-13. If the split window IR algorithm can not be applied due to poor quality moderate resolution  $t_{11\mu m}$  or  $t_{12\mu m}$  brightness temperatures the single-band fallback A-14 is used. Detailed algorithm flow chart descriptions are provided in the VIIRS Ice Quality/ST IP OAD [D42821].

## A.3.2 ALGORITHM INPUT

### A.3.2.1 VIIRS Data

The VIIRS data presented in Table A-2 are required input to the algorithm processing code.

**Table A-2. VIIRS data for the Surface Temperature IP**

<b>Input Data</b>	<b>Source of Data</b>	<b>Reference</b>
Instrument (Band) Quality	VIIRS SDR	[Y2479]
Granule Range Flag	Ice Quality Flags IP (formerly Ice Mask IP)	[D42821]
Brightness Temperature (M15, M16, I5)	VIIRS SDRs	[Y2479], [D43777]
Solar/Sensor Angles	VIIRS SDRs	[Y2479]
Ice Mask	Ice Quality Flags IP (formerly Ice Mask IP)	[D42821]
Ice Weights	Ice Weights IP	[D42821]
Aerosol Optical Thickness (AOT)	Aerosol Optical Thickness IP	[D39292]
Surface Temperature IP Coefficients	ST IP Regression Coefficients LUT	[D42821]

#### ***Instrument (Band) Quality***

The VIIRS EV\_375M SDR will contain band I5 quality flags at imagery pixel resolution. Pixels with bad quality will not be processed. A RED quality flag will be set for these pixels. The VIIRS EV\_750M SDR will contain band M15 and M16 quality flags at moderate pixel resolution. Imagery pixels nested within a moderate resolution pixel with bad quality will be processed by the fallback single band algorithm. A YELLOW quality flag will be set for these pixels.

#### ***Brightness Temperatures***

Brightness temperatures for the M15 and M16 bands are obtained from the VIIRS EV\_750M SDR. Brightness temperatures for the I5 band are obtained from the VIIRS EV\_375M SDR.

### ***Solar / Sensor Angles***

The sensor zenith angle is used in the split window algorithm (Equation A-6).

### ***Aerosol Optical Thickness***

Aerosol optical thickness is used to flag for degraded performance when slant path AOT > 1.0.

### ***Ice Quality Flags***

The VIIRS Ice Quality Flags IP [D42821] is expected to derive Cloud Quality, Sea Ice flag, Fresh Water Ice flag, and other quality flags used by the ST IP algorithm at imagery resolution.

### ***Surface Temperature IP Parameters***

The spectral fusion factor parameters will be used implicitly in the ST IP regression coefficients according to Equation A-13. The spectral fusion factor is a weight factor for combining the M15 and M16 BTs (c.f. Equation A-7) and it is not required to be determined explicitly for the regression retrieval of ST IP.

### ***Surface Temperature Coefficients***

The regression coefficients used in the split window and single band algorithms will be obtained from a pre-set ST IP Regression Coefficients LUT.

#### **A.3.2.2 Non-VIIRS Data**

The algorithm requires no input data from outside the VIIRS system.

### **A.3.3 THEORETICAL DESCRIPTION OF SURFACE TEMPERATURE IP RETRIEVAL**

#### **A.3.3.1 Physics of the Problem**

The physics of the ST IP retrieval are described in Section 3.3.1, in the EDR portion of this document.

#### **A.3.3.2 Mathematical Description of the Algorithm**

##### **A.3.3.2.1 Split Window Regression**

The VIIRS ST IP algorithm is based on statistical methods. Traditional statistical methods for satellite ST IP retrieval are linear multi-channel regression methods. The following regression methods are used in the VIIRS ST IP retrieval:

Split window (10.8 + 12  $\mu\text{m}$  bands, from AVHRR method, Yu et al., 1995) (VIIRS ST IP baseline algorithm):

$$\text{IST} = a_0 + a_1 T_{11} + \alpha_2 (T_{11} - T_{12}) + a_3 (\sec(z) - 1) \quad (\text{A-1})$$

One channel (12  $\mu\text{m}$  band). (VIIRS ST IP fallback algorithm):

$$\text{IST} = b_0 + b_1 T_{12} + b_2 (\sec(z) - 1) \quad (\text{A-2})$$

Satellite-measured radiance is a function of the atmospheric profiles and surface properties. For the IR window and water vapor channels, the radiance over oceans at the top of the atmosphere is mainly a function of the surface temperature and the temperature and moisture profiles. One can choose a few channels (e.g., 3 channels) for which only the main structures of the temperature and moisture profiles are required to obtain ice surface temperature.

##### **A.3.3.2.2 Calibrated TOA Brightness Temperatures**

The blackbody radiance (R) function is

$$R = 2 h \nu^3 / [c^2 (\exp\{-h\nu/kT\} - 1)] \quad (\text{A-3})$$

where  $\nu$  is the wavenumber ( $\text{cm}^{-1}$ ),  $h$  is the Planck constant,  $c$  is the speed of light,  $k$  is Boltzman's constant, and  $T$  is the temperature in Kelvin.

Equation A-3 can be written as

$$R = c_1 \nu^3 / [c^2 (\exp\{-c_2 \nu/T\} - 1)] \quad (\text{A-4})$$

where  $c_1$  and  $c_2$  are two blackbody constants equal to 0.01191071 and 1.438838 respectively using cgs units.

This can be solved for the brightness temperature ( $T$  or  $T_b$ ) to give:

$$T_b = c_2 v / \ln[1/(1 + c_1 v^3 / c^2 R)] \quad (\text{A-5})$$

### A.3.3.2.3 Fusion with Imagery Resolution Band

Note: In the following equations, we use a convention whereby quantities at imagery resolution are designated with lower case characters, quantities at moderate resolution are designated with upper case characters, and observed quantities are in italic font.

The purpose of achieving a fusion of the moderate resolution brightness temperatures with the imagery resolution brightness temperature is to be able to apply the split window algorithm at imagery resolution:

$$st = a_0 + a_1 t_{11} + \alpha_2 (t_{11} - t_{12}) + a_3 [\sec(z) - 1] \quad (\text{A-6})$$

where:

$st$  = Ice surface temperature (K) at imagery resolution

$t_{11}$  = M15 brightness temperature (K) at imagery resolution

$t_{12}$  = M16 brightness temperature (K) at imagery resolution

$z$  = Sensor zenith angle

$a_0, a_1, \alpha_2, a_3$  are the regression coefficients

In equation A-6, the  $_{11}$  and  $_{12}$  subscripts for the M15 and M16 bands are used to match the terms in the ST IP split window algorithm (Equation A-1) and the regression coefficients are identical to those for the IST algorithm.

To apply equation A-6, we must derive  $t_{11}$  and  $t_{12}$ , which are not directly observable by the VIIRS bands. To solve for these two unknowns, we use the observed brightness temperatures in the M15, I5, and M16 bands, and make the following assumptions:

1) The brightness temperature in the LWIR imagery band (I5) can be written as a linear combination of the brightness temperatures in the moderate resolution LWIR bands (M15 and M16):

$$t_I = f t_{11} + (1 - f) t_{12} \quad (\text{A-7})$$

where:

$t_I$  = I5 brightness temperature (K) at imagery resolution

and the spectral fusion factor,  $f$ , which is defined by equation A-7, is in general a function of  $R$ , the source radiance spectrum.

The spectral fusion factor can be rigorously determined from the spectral response functions, as part of the calibration process. This is determined statistically from equation A-5:

$$f = (t_I - t_{12}) / (t_{11} - t_{12}) \quad (\text{A-8})$$

where:

$$t_I = c_2 v_I / \ln(1 + c_1 v_I^3 / R_I) , \text{ etc.} \quad (\text{A-9})$$

2) The brightness temperature difference,  $t_{11} - t_{12}$ , is primarily determined by atmospheric conditions that are stable on a spatial scale of a few km. This allows us to reliably approximate the brightness temperature difference at imagery resolution as the difference in the nearest moderate resolution pixel:

$$\delta = D \quad (\text{A-10})$$

where:

$$\delta = t_{11} - t_{12} \quad (\text{A-11})$$

$$D = T_{11} - T_{12} \quad (\text{A-12})$$

$\delta$  and  $D$  are the differences in M15 and M16 brightness temperatures for the moderate and imagery pixels respectively.

3) Applying the approximation in Equation A-10 to Equations A-7 and A-8,  $t_{11}$  can be expressed as  $t_{11} = t_l - (1-f)D$ . Substituting the expression for  $t_{11}$  into Equation A-6 and applying the A-10 approximation, Equation A-6 can be rearranged into

$$st = a_0 + a_1 t_l + a_2 D + a_3 [\sec(z) - 1] \quad (\text{A-13})$$

where  $st$  is the Ice surface temperature IP (K),  $t_l$  is the VIIRS I5 brightness temperature (K),  $D = T_{11} - T_{12}$  (K) is the difference in M15 and M16 brightness temperatures all at imagery resolution,  $z$  is the sensor zenith angle of the imagery, and  $a_0, a_1, a_2, a_3$  are the regression coefficients with  $a_2$  defined as  $a_2 = a_1(1 - f) + \alpha_2$  and  $f$  is the Spectral Fusion Factor defined by Equation A-7.

Equation A-13 is a linear regression equation to be use for the baseline 2-band split window algorithm in the ST IP retrieval at imagery pixels. It is noted that the spectral fusion factor is not needed explicitly for the algorithm.

#### **A.3.3.3 Single Band Fallback**

The split window algorithm cannot be applied if the M15 or M16 data are of poor quality or missing. In that case, a single band fallback algorithm will be applied:

$$st = b_0 + b_1 t_l \quad (\text{A-14})$$

with the regression coefficients  $b_0$  and  $b_1$ , and a quality flag will be attached.

#### **A.3.3.4 Archived Algorithm Output**

Surface Temperature will be produced at imagery resolution as the Surface Temperature IP. The IP is used as input to the VIIRS Ice Concentration software unit [Y3235]. It can be archived as a P<sup>3</sup>I product. Currently, the IP will not be written for pixels outside of the Horizontal Coverage range for sea ice or fresh water ice. If there is interest in a P<sup>3</sup>I product outside of the ice zones, the algorithm can be implemented over a wider region.

#### **A.3.3.5 Variance and Uncertainty Estimate**

The Surface Temperature IP is not a system level requirement and therefore does not have a system specification. Surface Temperature IP performance requirements are thus driven by the system specifications for the Sea Ice Characterization EDR [D41063]. Surface temperature IP errors were estimated in Phase I as part of the error budget process for the Imagery Sea Ice products [D43767]. Performance estimates were derived as follows:

The split-window Ice Surface Temperature algorithm was applied to MODIS Airborne Simulator (MAS) scenes at a 50 meter pixel resolution. Brightness temperatures in MAS

bands 45 (11  $\mu\text{m}$ ) and 46 (12  $\mu\text{m}$ ) were calculated from the unperturbed TOA radiances in those bands, and used as input data to the algorithm. The retrieved surface temperatures were adopted as “truth”. The 50 meter truth was aggregated to VIIRS imagery pixel sizes at nadir (8 x 8 aggregation to 0.4 km pixels). The aggregated temperatures were adopted as VIIRS “truth”.

The MAS TOA radiances were then aggregated to VIIRS pixel size. A proxy for the VIIRS I5 band radiance was made from the average of the band 45 and 46 radiances. The VIIRS model radiances were perturbed by our models for sensor noise and calibration bias. A 0.5% calibration bias was applied to all radiances. Sensor noise models for VIIRS bands M15 (11  $\mu\text{m}$ ), M16 (12  $\mu\text{m}$ ), and I5 (11.45  $\mu\text{m}$ ) were applied to the corresponding radiances. The perturbed radiances were converted to brightness temperature, and used as input data to the Surface Temperature IP algorithm.

Surface Temperature IP accuracy, precision, and uncertainty errors were calculated from comparison of the retrieved surface temperature to the “truth”. At nadir, these errors are 0.278 K in accuracy and 0.378 K in precision. At edge of scan, the precision error is 0.508 K.

It may seem at first glance that this performance is much better than would be expected from the NEdT specification for the I5 band (c.f. Table A-1). There are two reasons for this:

- 1) The NEdT specification for band I5 is at a reference temperature ( $T_{\text{typ}}$ ) of 210K. Surface temperatures in regions where we need performance (the marginal ice zones) are ~ 270K, where NEdT is significantly smaller.
- 2) NEdT performance is better than specification, since our specification includes margin. NEdT performance for the three thermal bands used by the algorithm is shown in Figure A-4.

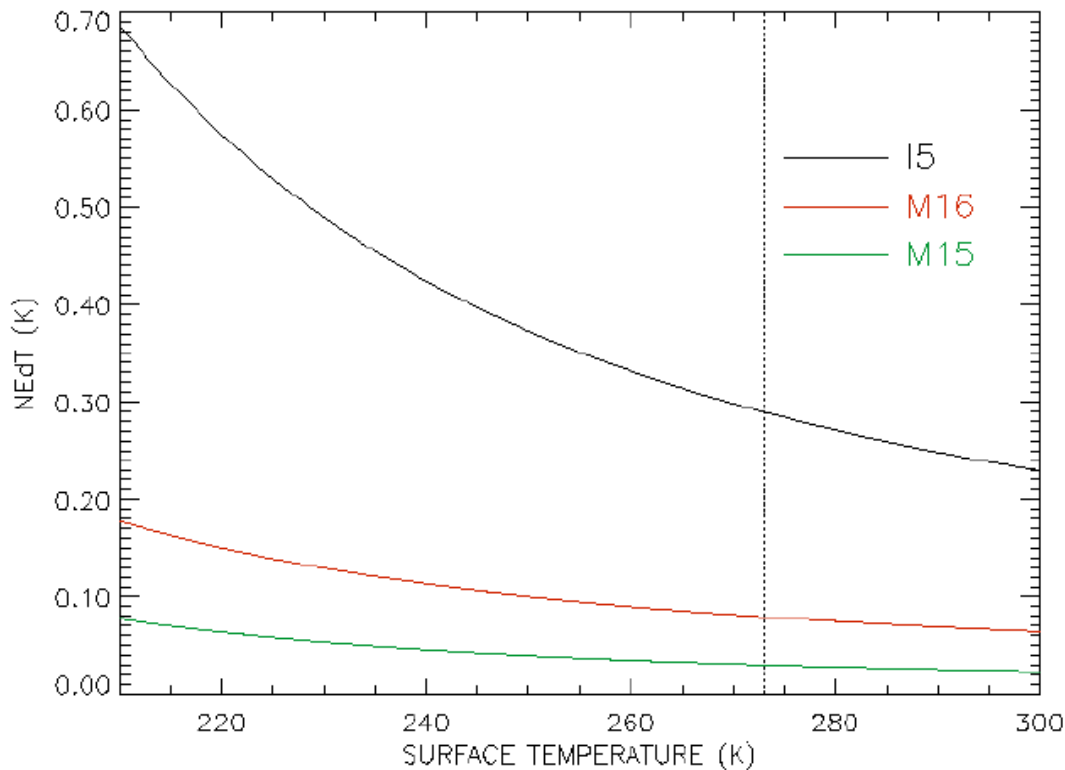


**Figure A-1. NEdT performance estimates for bands I5, M15, and M16**

At the ice/water temperature boundary ( $\sim 273$  K, indicated by the vertical dotted line in the figure), band I5 NEdT performance is 0.289 K. This is somewhat smaller than our derived precision error in Phase I (0.378K at nadir). We assume that the additional derived error is due to band misregistration and/or atmospheric variance, and that the error derived in Phase I from MAS data is still a good estimate of the Surface Temperature IP error in the marginal ice zones.

#### A.3.4 ALGORITHM SENSITIVITY STUDIES

We identify the following factors as possibly contributing to the total error budget for the Surface Temperature IP

- Sensor noise
- Calibration
- MTF
- Band Registration
- Atmospheric Correction

**Sensor Noise:** Sensor noise is characterized by the NEdT, as discussed in Section A.3.3.5.

**Calibration:** We applied a calibration bias of 0.5% to the brightness temperature, as discussed in Section A.3.3.5.

**MTF:** MTF smearing of the radiances will alias real horizontal variability into errors in measured reflectance and/or temperature for a given pixel. We have not quantified this error yet. Our sensitivity study with the MAS scene (Section A.3.3.5) will have included MTF effects in the total measured error.

**Band Registration:** Band-to-band registration errors will also alias horizontal variability into measurement error. These errors only apply to the split window retrieval, which uses more than one band. Our sensitivity study with the MAS scene (Section A.3.3.5) will have included band misregistration effects in the total measured error. If band misregistration is determined to be a significant error source, we can always use the single band algorithm. Such a determination will have to await validation with actual NPOESS Preparatory Program (NPP)/VIIRS data.

**Atmospheric Correction:** Atmospheric correction errors are typically perturbations in derived brightness temperature caused by water vapor and aerosols. These errors, discussed in Section 3.3.4, are generally not expected to be important for most cases of retrievals in polar regions. An additional source of atmospheric error is the spatial variability of water vapor at moderate versus imagery resolution.

## **A.3.5 PRACTICAL CONSIDERATIONS**

### **A.3.5.1 Numerical Computation Considerations**

Because all coefficients are pre-computed and stored in LUTs, the algorithm will run quickly and efficiently.

### **A.3.5.2 Programming and Procedural Considerations**

The algorithm requires data from the Build SDR Module, the Snow/Ice Module, the Aerosol Module, and the Cloud Module.

### **A.3.5.3 Quality Assessment and Diagnostics**

Pixel-based quality flags are provided which indicate the confidence in the IP. These will include quality flags for pixels containing bad data. A complete description of the quality flags and detailed format information is provided in the Operational Algorithm Description Document for the VIIRS Sea Ice Quality/Surface Temperature IP [D42821].

#### **A.3.5.4 Exception Handling**

The process will apply the pre-computed coefficients for all imagery resolution pixels containing good data. In the case that the co-spatial moderate resolution pixel contains bad data, the algorithm will apply the single band algorithm, and flag the pixel.

### **A.3.6 ALGORITHM VALIDATION**

#### **A.3.6.1 Pre-Launch Validation**

Pre-launch validation of the IST algorithms has been discussed in Section 3.6.1. Validation of the additional spectral and spatial functions used by the ST IP algorithm will be made from VIIRS EDU observed properties.

#### **A.3.6.2 Post-Launch Validation**

Post-launch validation of the IST algorithms has been discussed in Section 3.6.2. Validation of the additional spectral and spatial functions used by the ST IP algorithm will be made from NPP/VIIRS data.

#### A.4.0 ASSUMPTIONS AND LIMITATIONS

The ST IP algorithm is subject to the same assumptions and limitations as the IST algorithm (Section 4.0 of this document). The only additional assumption is that the water vapor correction at imagery resolution is sufficiently close to the correction at moderate resolution. By sufficiently close, we mean that the additional error caused by variation in water vapor on a spatial scale less than  $\sim 1\text{km}$  is small compared with the error in the split window IST retrieval.

## A.5.0 REFERENCES

- Berk, A., L. S. Bernstein, and D. C. Robertson (1987). MODTRAN: A moderate resolution model for LOWTRAN. Rep. GLTR-89-0122, Burlington, MA: Spectral Sciences, Inc.
- Cornette, W. M., P. K. Acharya, D. C. Robertson, and G. P. Anderson (1994). Moderate spectral atmospheric radiance and transmittance code (MOSART). Rep. R-057-94(11-30), La Jolla, CA: Photon Research Associates, Inc.
- Kneizys, F. X., E. P. Shettle, L. W. Abreu, J. H. Chetwynd, G. P. Anderson, W. O. Gallery, J. E. A. Selby, and S. A. Clough (1988). Users guide to LOWTRAN7. Rep. AFGL-TR-88-0177, Bedford, MA: Air Force Geophys. Lab.
- Yu, Y., D. A. Rothrock, and R. W. Lindsay (1995). Accuracy of sea ice temperature derived from the advanced very high resolution radiometer. *J. Geophys. Res.*, 100, 4525-4532.